ELECTROSTATIC DROPLET MANIPULATION USING ELECTRET AS A VOLTAGE SOURCE

Tianzhun Wu, Yuji Suzuki, and Nobuhide Kasagi

Department of Mechanical Engineering, The University of Tokyo

Hongo, Bunkyo-ku, Tokyo 113-8656, Japan

ABSTRACT

A novel low-voltage electrostatic droplet manipulation method, liquid dielectrophoresis on electret (L-DEPOE) is proposed. By using electret as a voltage source, a dielectric droplet can move between two electrodes by switching an external capacitor. A circuit model is developed to predict the electrostatic force acting on the droplet and the droplet motion. A prototype device has been microfabricated using glass substrates with ITO electrodes and CYTOP electret. Parylene protection layer on the top of CYTOP prevents charge decay of the electret. It is demonstrated that the silicone oil droplet is moved by switching the capacitor using a 5 V signal, which is much smaller than the voltage required for electrowetting on dielectrics (EWOD).

1. INTRODUCTION

Recently, electrowetting on dielectrics (EWOD) attracts much interest in droplet manipulation for Lab-On-Chip and optical applications [1, 2]. In EWOD, external voltage is employed to change the contact angles of aqueous liquid on electrodes with dielectric coating, and the surface tension acting on the liquid moves/deforms the droplet. However, the required voltage for EWOD devices is usually 20-80 V, which limits the their applications particularly in integrated microfluidic systems. By using very thin (~70 nm) and very high dielectric constant (~180) materials, a significant contact angle change can be achieved with voltages as low as 15 V [3], which is the minimum driving voltage ever reported. Limited by contact angle saturation and dielectric strength of the thin coating film [4], it is not straightforward to reduce the voltage further.

On the other hand, when liquid is subjected to a non-uniform electric field, the molecules form dipoles and net electrostatic force is induced, leading to the motion of liquid. This phenomenon is called "Liquid DEP" [5]. For a parallel capacitor, as shown in Fig. 1, the electric fringe field can be used to move liquid near its edge, where the individual molecule of dielectric liquid is polarized. Net electrostatic force is exerted on the dipole, causing suction of the liquid into the capacitor gap. This phenomenon was first observed by Pellat in 1895. The Liquid DEP can exert both on dielectric and conductive liquid [6], but usually high AC voltage (>200 V_{rms}) is needed. Therefore, from the viewpoint of applications with CMOS circuits, low-voltage liquid manipulation methods are desired.

In the present study, we employ electret as a voltage source for droplet manipulation. Electret is dielectric material with quasi-permanent charge, and used for MEMS microphone [7] and micro power generator [8-10]. Tsutsumino et al.[10] found that a MEMS-compatible amorphous perfluoropolymer CYTOP (CTL-809M, Asahi

Glass Co., Ltd.) provides high surface charge density up to 1.37 mC/m^2 (-1100 V on 15 µm-thick film CYTOP) and long-term stability.

Although surface voltage of electret produced by the trapped charge inside can be higher than -1000 V, the surface voltage cannot be changed with external signals. Thus, we employ relays/switches to connect/disconnect external capacitors, and thereby change the electrostatic potential distribution for droplet manipulation. Since high-speed electric relays or switches can be driven with low voltage (typically 3-5 V) and low power consumption, it is possible to develop a low-voltage droplet manipulation device in conjunction with electrets. In this report, we describe the actuation principle of our liquid-DEP-on-electret (L-DEPOE) device.

2. L-DEPOE MODEL AND SIMULATION

A typical L-DEPOE device using a relay/switch is schematically shown in Fig. 2. The system consists of a MEMS fluidic device and an external circuit. A dielectric droplet partially occupies two bottom electrodes, dividing the fluidic channel into 4 parts. Each part can be modeled with an equivalent capacitor formed by the electret film ($C_{e1}\sim C_{e4}$) and air or liquid medium between the electret and the bottom electrodes ($C_1\sim C_4$). When one of the bottom electrodes is connected to an external capacitor switched by electric relays (e.g., PhotoMOS relays), Liquid DEP force F_e acts on the droplet due to asymmetry of the circuit, and then the droplet moves from one side to the other.
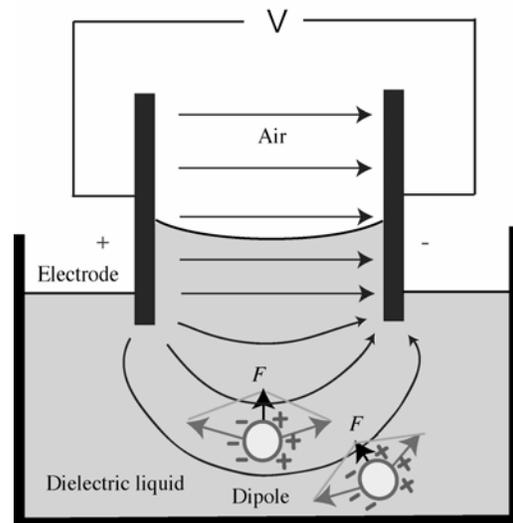
Figure 1: Concept of liquid DEP [5] .
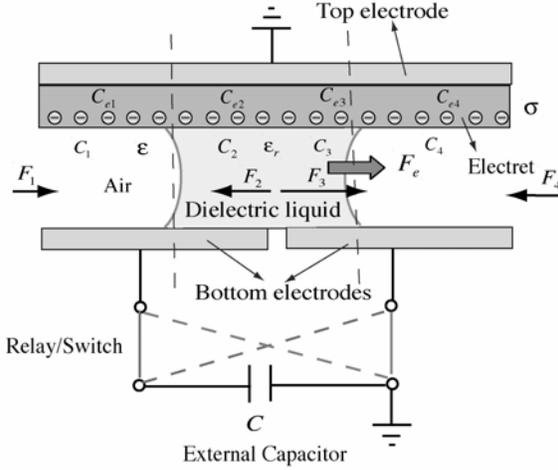
Figure 2: Schematic of a microfluidic device using liquid DEP on electret (L-DEPOE). One external capacitor can be switched to one of the bottom electrodes by electric relays/switches.
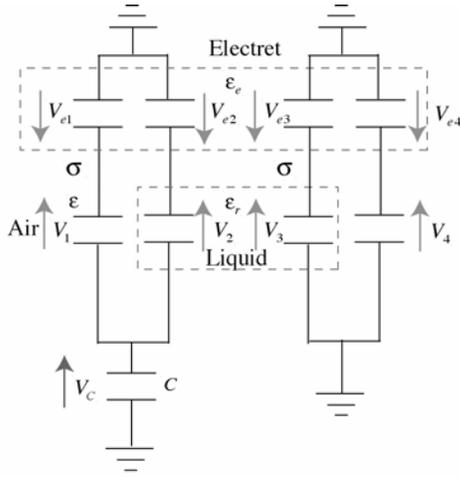
Figure 3: Circuit model of L-DEPOE.

Figure 3 shows a simplified circuit model of the L-DEPOE device. σ and C are respectively the surface charge density of electret and the external capacitor. $C_{e1} \sim C_{e4}$ represent equivalent capacitances of the electret film, while C_1, C_4 and C_2, C_3 are respectively capacitances corresponding to the air and liquid medium between the electret surface and the bottom electrode. $C_1 \sim C_4$ are functions of the right electrode width x occupied by the droplet. Voltages on these capacitors $V_1 \sim V_4$ and the electrostatic potential can be calculated as the following procedure.

By applying the Gauss's law to the surface of electret film, the following equations can be obtained.

$$-\varepsilon_e \frac{V_{e1}}{s} - \varepsilon \frac{V_1}{h} = \frac{\sigma}{\varepsilon_0}, \tag{1}$$

$$-\varepsilon_e \frac{V_{e2}}{s} - \varepsilon_r \frac{V_2}{h} = \frac{\sigma}{\varepsilon_0}, \tag{2}$$

where ε_e, ε, and ε_r are relative permittivity respectively for electret, air, and liquid, while ε_0 is the permittivity of

vacuum. Parameters s and h are the thickness of the electret film and the gap height.

With the Kirchhoff's second law, we get

$$V_{e1}-V_1-V_C=0, \tag{3}$$
$$V_{e2}-V_2-V_C=0, \tag{4}$$

According to the charge conservation for the bottom electrode on the left hand side,

$$C_1V_1+C_2V_2-CV_C=0. \tag{5}$$

From Eqs. (1)~(5), V_1, V_2, V_{e1}, V_{e2}, and V_C can be obtained. Similarly, potentials for the right hand side (V_3, V_4, V_{e3}, V_{e4}) are solved. The total electric potential energy W_C stored in this system is expressed as

$$W_C = \frac{1}{2}\sum_{k=1}^{4} C_{ek}V_{ek}^2 + \frac{1}{2}\sum_{k=1}^{4} C_k V_k^2 + \frac{1}{2}CV_C^2. \tag{6}$$

Based on the principle of minimum energy, the system changes toward its minimum energy state. The electrostatic force F_e on the droplet is obtained by taking the derivative of W_C with respect to x as

$$F_e = -\frac{dW_C(x)}{dx}. \tag{7}$$

With this electrostatic force, the droplet moves until the system potential energy reaches its minimum value. When the contact angles for the droplet remain constant during the motion, the dumping force due to viscosity of the liquid is assumed to be

$$F_d = -\frac{\mu \cdot 2A}{h/2}\frac{dx}{dt} = -\frac{4\mu A}{h}\frac{dx}{dt}, \tag{8}$$

where μ and A are respectively the viscosity and the contact area with the electret surface and the bottom electrodes. Thus, the equation of motion becomes a second-order differential equation:

$$m\frac{d^2x}{dt^2} = -\frac{4\mu A}{h}\frac{dx}{dt} - \frac{dW_C(x)}{dx}, \tag{9}$$

where m is the mass of the droplet.

Analytical solution of Eq. (9) can be easily obtained with given parameters. In the actual design described later, whole inner surfaces are coated with parylene-C. Therefore, the model shown in Fig. 3 should be modified with additional equivalent capacitors. But, the calculation procedure of the electrostatic force and the droplet motion is similar.

Figure 4 shows a group of the computational results with parameters used in the experiments and the external capacitance C is systematically changed. Upon switching the capacitor, the voltage on the external capacitor jumps up at t=0, followed by gradual reduction. Smaller external capacitor leads to higher voltage on the capacitor. The droplet velocity is almost constant during the motion, and is decreased with increasing external capacitance. The droplet velocity at C=1 pF in this simulation is about 4 mm/s.

4. FABRICATION PROCESS

The cross-sectional view of our early prototype is shown in Fig. 5. Pyrex wafers are used as the substrate for both top and bottom parts. To observe the droplet motion under a microscope, ITO (Indium-Tin-Oxide) electrodes are employed. Parylene-C is deposited on the top electret film to reduce charge decay, and also on the bottom electrodes to
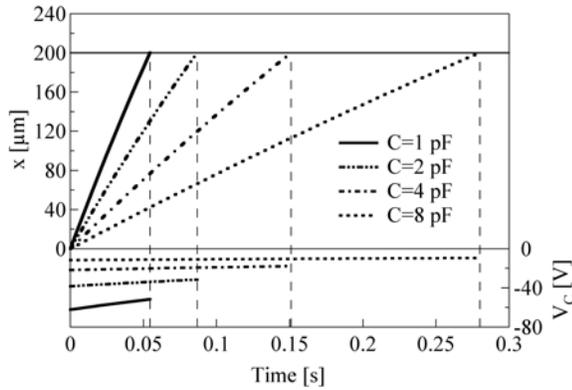
Figure 4: Computational results for droplet motion and the voltage on the external capacitor.
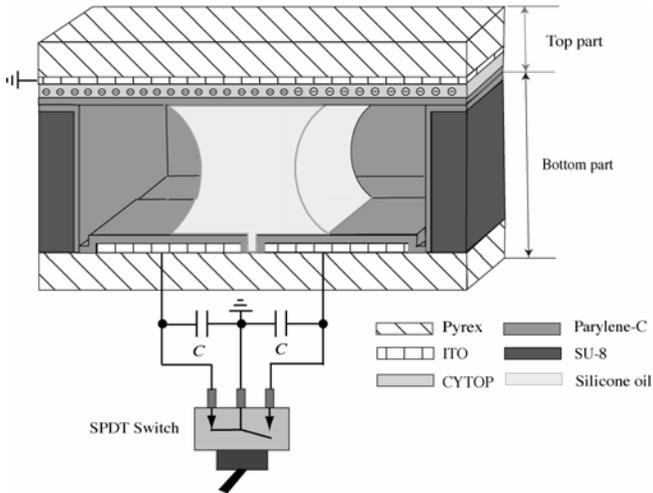
Figure 5: Structure of the prototype for L-DEPOE.

Figure 6: Process flow for the prototype.

prevent them from liquid contamination. SU-8 is used to define the gap between the top and bottom substrates, and silicone oil is used as the dielectric droplet. A single-pole-double-throw (SPDT) manual switch or electric relays driven by low-voltage power supply can be used to switch the external capacitor to one of the bottom electrodes, whereas the other bottom electrode is grounded.

The main fabrication process flow is shown in Fig. 6. For the top part, 200 nm-thick ITO is sputtered on a Pyrex substrate, and then 15 µm-thick CYTOP CTL-809M (Asahi Glass Co., Ltd.) is spun on. CYTOP is cured at 185 °C for 1.5 hours, followed by 5 µm-thick parylene-C deposition on the CYTOP film. Finally, corona charging (-10 KV needle voltage and -600 V grid voltage [10]) is employed to implant charge into CYTOP through parylene-C coating.

Process flow for the bottom part also starts with the deposition of 200 nm-thick ITO film on a Pyrex wafer with sputtering. The ITO film is then patterned to form the bottom electrodes using standard lithography. The electrodes used in the present experiments are 2 mm × 0.5 mm with the gap of 30 µm (Fig. 7). Next, HMDS is applied to increase the adhesion between Pyrex and SU-8, and then SU-8 100 (Microchem Corp.) is dispensed and spun with the spin speed of 2300 rpm, followed by a soft bake, UV

exposure, a post-exposure bake and development. After rinsing and drying, 5 µm-thick parylene-C is deposited.

A simple fixture is used to assemble the top and bottom parts after the silicone oil droplet (Shinetsu Silicone, KF-96, 10 cP) is injected by a nanoliter-range syringe.

5. EXPERIMENTAL RESULTS

The prototype device is placed under the microscope (Olympus IX71) equipped with a high-speed camera (Phantom V7.1, Vision Research Inc). Two separate experiments have been made with different devices to switch the external capacitor.

For the first experiment, a SPDT manual switch is employed. Snap shots for droplet are shown in Fig. 7. The electret surface voltage is about –1.1 KV (σ=-1.37 mC/m^2), and the external capacitance C including parasitic capacitance is 3 pF. By manually switching the external capacitor, the droplet moves between the two electrodes. For Figs. 7a-c, the right electrode is connected to the external capacitor while the left electrode is grounded, thus the droplet moves from right to left. On the other hand, for Figs. 7d-f, the left electrode is connected to the external capacitor, thus the droplet goes back to the right. The time trace of the droplet motion is plotted in Fig. 8. The droplet initial velocity for Figs. 7a-c is 75 µm/s, about 40 times slower than expected, while the initial velocity for Figs. 7d-f is 120 µm/s, about 7 times slower than expected.

For the second experiment, a SPDT signal relay ATX209 (TX2-5V, 2 Form C, Matsushita Electric Works, Ltd.) driven with 5 V and 30 mA is employed. Its operation time is about 2 ms. External capacitance is about 6 pF. Time trace of the droplet motion is shown in Fig. 9. Again, the droplet moves between the electrodes by switching the external capacitor using the signal relay. In this case, the droplet initial velocity is about 300 µm/s, about 2 times slower than the estimated value.
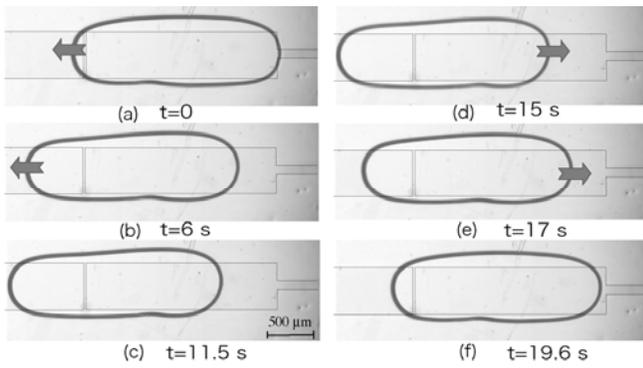
Figure 7: Snap shots of the droplet motion for the device with a manual SPDT switch. At t=0 and 15 s, the switch is flipped to drive the droplet.
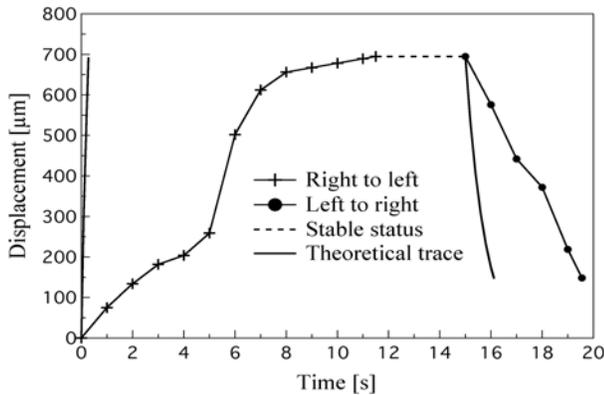
Figure 8: Time trace of the droplet motion for the device with a manual SPDT switch.
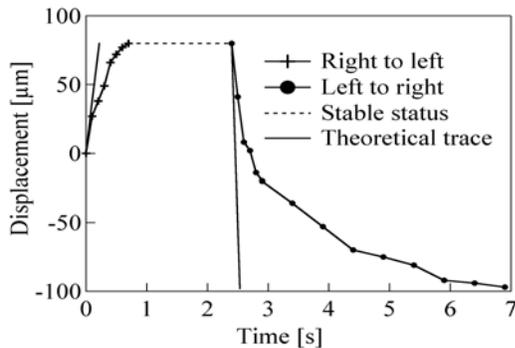
Figure 9: Time trace of the droplet position for the device with a signal relay.

It is now clear that the droplet motion can be manipulated with the present L-DEPOE scheme. However, as shown in Figs. 8 and 9, the droplet velocity in our early prototype is much slower than expected, especially for a long distance or a long traveling time. We conjectured that this is due to the finite leakage current inside the manual switch and signal relay. Since their resistances are respectively 5 GΩ and 7 GΩ, the discharging time constant for the RC circuit is on the order of mili-second, which is much smaller than the traveling time. Therefore, the voltage on the external capacitor V_C is markedly reduced due to the leakage current, leading to the slower motion. The droplet speed should be improved by using relays with larger resistance.

6. CONCLUSION

In the present study, we propose a versatile low-voltage droplet manipulation method using electret as a voltage source. An early prototype of droplet manipulation device based on liquid DEP on electret (L-DEPOE) has been successfully developed. We have demonstrated that a silicone oil droplet can move between two electrodes by switching an external capacitor with a voltage signal as low as 5 V.

REFERENCES

[1] S. Cho, H. Moon, and C. Kim, "Creating, Transporting, Cutting, and Merging Liquid Droplets by Electrowetting-Based Actuation for Digital Microfluidic Circuits", *J. Microelectromech. Syst.*, vol. 12, pp. 70-80, 2003.

[2] F. Krogmann, W. Monch, and H. Zappe, "A MEMS-based Variable Micro-lens System", *J. Opt. A*, vol. 8, pp. S330-336, 2006.

[3] H. Moon and S. Cho, "Low voltage electrowetting-on-dielectric", *J. Appl. Phys.*, vol. 92, pp. 4080–4087, 2002.

[4] B. Shapiro, H. Moon, R. Garrell, and C. Kim, "Equilibrium Behavior of Sessile Drops under Surface Tension Applied External Fields, and Material Variations", *J. Appl. Phys.*, vol. 93, pp. 5794-5811, 2003.

[5] T. Jones, "Liquid Dielectrophoresis on the Microscale", *J. Electrost.*, vol. 51-52, pp. 290-299, 2001.

[6] T. Jones, "On the Relationship of Dielectrophoresis and Electrowetting", *Langmuir,* vol. 18, pp. 4437-4443, 2002.

[7] W. Hsieh, T. Yao, and Y. Tai, "A High Performance MEMS Thin-film Teflon Electret Microphone", *Transducers '99*, Sendai, pp. 1064-1067, 1999.

[8] J. Boland, C. Chao, Y. Suzuki, and Y. Tai, "Micro Electret Power Generator", *IEEE Int. Conf. MEMS'03*, Kyoto, pp. 538-541, 2003.

[9] J. Boland, J. Messenger, H. Lo, and Y. Tai, "Arrayed Liquid Rotor Electret Power Generator Systems", *IEEE Int. Conf. MEMS'05*, Miami, pp. 618-621, 2005.

[10] T. Tsutsumino, Y. Suzuki, N. Kasagi, and Y. Sakane, "Seismic Power Generator Using High-performance Polymer Electret", *IEEE Int. Conf. MEMS'06*, Istanbul, pp. 98-101, 2006.